

Fits of $SU(3)$ $N_f = 8$ data to dilaton-pion effective field theory

Maarten Golterman*

Department of Physics and Astronomy, San Francisco State University

San Francisco, CA 94132, USA

E-mail: maarten@sfsu.edu

Yigal Shamir

Raymond and Beverly Sackler School of Physics and Astronomy, Tel Aviv University

69978 Tel Aviv, Israel

E-mail: shamir@post.tau.ac.il

We report on fits of the $SU(3)$ $N_f = 8$ LSD spectral data to chiral perturbation theory with a dilatonic meson. These fits confirm that current simulations are in the “large-mass” regime, with approximate hyperscaling as the leading mass dependence. We find that the leading-order effective field theory describes the data well. In particular, the effective field theory allows us to understand the staggered taste splitting, explaining the pattern observed in the LSD data, which looks different from QCD.

37th International Symposium on Lattice Field Theory - Lattice2019

16-22 June 2019

Wuhan, China

*Speaker.

1. Introduction

Numerical simulations of the $SU(3)$ gauge theory with $N_f = 8$ flavors of fundamental fermions show that the spectrum of the theory behaves quite differently from the spectrum of a similar theory with far fewer (light) flavors, such as QCD [1, 2] (see also Ref. [3]). The salient differences are three-fold: (1) the 8-flavor theory contains a stable flavor-singlet 0^{++} state which, at the fermion masses explored in the simulations, is light and approximately degenerate with the pseudo-scalar Nambu–Goldstone (NG) bosons associated with chiral symmetry breaking (“pions”), (2) dimensionless ratios of hadronic quantities are nearly independent of the fermion mass (over a range of fermion masses differing by factors up to 7), and (3) a taste-breaking pattern that looks very different from that in QCD (staggered fermions were used for the simulations of Refs. [1, 2]).

While the simulations indicate that the 8-flavor theory breaks chiral symmetry also in the chiral limit, with the light 0^{++} state in the spectrum standard chiral perturbation theory (ChPT) clearly cannot be used as a low-energy effective theory. Instead, it should be expanded to include the physics of the light scalar state, and, if this is to be done systematically, a guiding principle that leads to a power counting scheme is required. Such an effective theory was proposed based on the assumption that the light scalar is an approximate NG boson for the breaking of scale invariance, which is assumed to be small because of the proximity of the 8-flavor theory to the conformal window. In Refs. [4, 5, 6, 7], it is assumed that the difference of the number of flavors, N_f , with the critical value $N_f^*(N_c)$ at which theory enters the conformal phase in which the theory develops an infra-red fixed point (IRFP) can be used as an expansion parameter. More precisely, the small parameter is $n_f - n_f^*$, with $n_f = \lim_{N_c \rightarrow \infty} N_f/N_c$ and $n_f^* = \lim_{N_c \rightarrow \infty} N_f^*(N_c)/N_c$, where the Veneziano limit $N_c, N_f \rightarrow \infty$ with fixed ratio is taken. As explained in detail in Refs. [4, 5], this assumption allows us to augment standard ChPT with an effective field describing the light scalar, which we will refer to as the dilatonic meson, or dilaton.¹ We will refer to this extension of ChPT as dChPT.

Here, we test tree-level dChPT on the published data of Ref. [2], as a natural first step. (With the currently attained numerical precision, NLO effects are unlikely to be quantitatively accessible.) Some tree-level tests have been carried out in Ref. [8]; the results we report below are in agreement with those reported in Ref. [8]. A new result is our exploration of taste-breaking effects, for which we refer to Sec. 3 below. We emphasize that all results reported here are based on fits of the data as published in Ref. [2]. No correlations have been taken into account, and all results should be considered preliminary. Work on a more complete analysis of the numerical data is in progress [9].

2. dChPT at tree level

The leading-order dChPT lagrangian is [4]

$$\mathcal{L} = \frac{1}{4} \hat{f}_\pi^2 e^{2\tau} \text{tr}(\partial_\mu \Sigma^\dagger \partial_\mu \Sigma) + \frac{1}{2} \hat{f}_\tau^2 e^{2\tau} \partial_\mu \tau \partial_\mu \tau - \frac{1}{2} \hat{f}_\pi^2 \hat{B}_\pi e^{(3-\gamma_*)\tau} m \text{tr}(\Sigma + \Sigma^\dagger) + \hat{f}_\tau^2 \hat{B}_\tau e^{4\tau} c_1 \left(\tau - \frac{1}{4} \right). \quad (2.1)$$

Here τ is the field describing the dilatonic meson, and $\Sigma = \exp(2i\pi/\hat{f}_\pi)$ is the usual field describing the pions; \hat{f}_π , \hat{f}_τ , \hat{B}_π , and \hat{B}_τ are low-energy constants, and γ_* is the value of the mass-anomalous

¹For more on the assumptions underlying our framework, see Ref. [7].

dimension at the nearby IRFP [4, 6]. The small parameters are the fermion mass $m > 0$, and $c_1 \propto n_f - n_f^*$. At fixed n_f , the dilatonic meson τ decouples in the $m \rightarrow 0$ limit, in which the pions are described by ordinary ChPT (for 8 light flavors). For larger values of m , there exists a “large-mass” regime which exhibits approximate hyper-scaling; dChPT is applicable as long as $c_1 \log m \ll 1$ [7]. The τ field has been shifted such that $v \equiv \langle \tau \rangle = 0$ for $m = 0$.

First, the classical potential is minimized by setting $\Sigma = 1$, and solving

$$\frac{m}{c_1 \hat{M}} = v(m) e^{(1+\gamma_*)v(m)}, \quad \hat{M} = \frac{4 \hat{f}_\tau^2 \hat{B}_\tau}{\hat{f}_\pi^2 \hat{B}_\pi N_f (3 - \gamma_*)}, \quad (2.2)$$

for $v(m)$. Note that this is an $O(1)$ relation, because both m and c_1 are small, and assumed to be of the same order. Some of the tree-level predictions following from Eqs. (2.1) and (2.2) are

$$\begin{aligned} F_{\pi,\tau} &= \hat{f}_{\pi,\tau} e^{v(m)}, \\ M_\pi^2 &= 2 \hat{B}_\pi m e^{(1-\gamma_*)v(m)}, \\ M_\tau^2 &= 4 c_1 \hat{B}_\tau e^{2v(m)} (1 + (1 + \gamma_*)v(m)). \end{aligned} \quad (2.3)$$

These results can be combined into the relations

$$\begin{aligned} M_\pi^2 F_\pi^{\gamma_* - 1} &= C m, \\ \frac{m}{F_\pi} &= D_2 \frac{M_\pi^2}{F_\pi^2} \exp\left(D_1 \frac{M_\pi^2}{F_\pi^2}\right), \\ \hat{f}_\pi &= (C D_2)^{1/\gamma_*}, \\ v(m) &= \frac{D_1}{\gamma_*} \frac{M_\pi^2}{F_\pi^2}, \end{aligned} \quad (2.4)$$

where C and $D_{1,2}$ are combinations of low-energy constants, including γ_* .

Assuming that the lattice spacing a does not depend on m , we can fit the first two relations (the second relation is in terms of dimensionless ratios, so the assumption is not needed in that case). Preliminary results are, in units of the lattice spacing²

$$\begin{aligned} \gamma_* &= 0.936(19), & C &= 1.93(6), \\ D_1 &= 0.22(3), & \log D_2 &= -8.8(5). \end{aligned} \quad (2.5)$$

From the last line of Eq. (2.4) we then find that $a \hat{f}_\pi \sim 0.0006$. This is much smaller than the computed values of $a F_\pi$, which range from 0.021 to 0.053 for fermion masses between $am = 0.00125$ and $am = 0.00889$. This large difference is explained by the factor $e^{v(m)}$ in the first line of Eq. (2.3). These factors thus range between about 35 and 90, indicating that the numerical simulations of Refs. [1, 2] are in the “large-mass” regime [7], where the factor $e^{(1+\gamma_*)v(m)}$ dominates over the factor $v(m)$ in Eq. (2.2). In this regime, the theory exhibits approximate hyperscaling. Figure 1 shows that results for the ratios of masses and F_π obtained by Ref. [2] are consistent with approximate hyperscaling as predicted by dChPT. Needless to say, this behavior is quite different from that in QCD. Since \hat{B}_π is by construction independent of m , we can test the independence of

²Early results indicate that proper correlated fits lead to results consistent with Eq. (2.5) with a good fit quality [9].

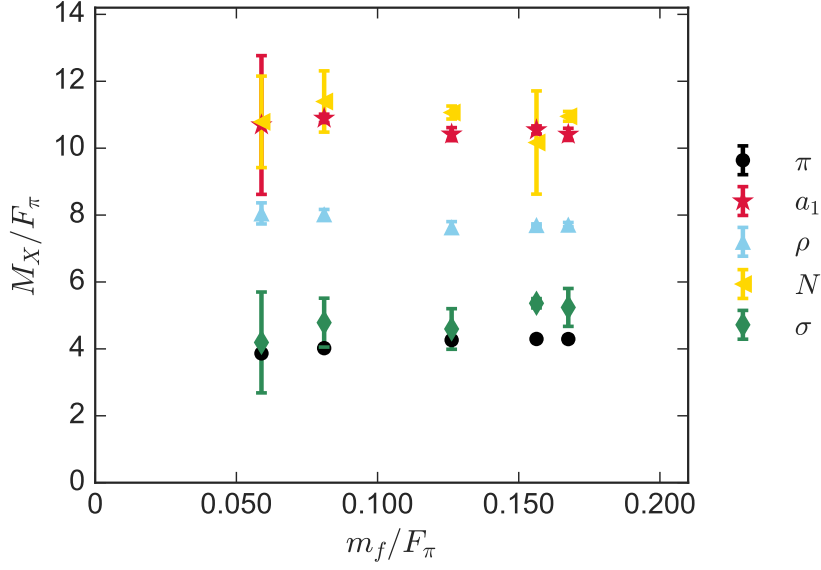


Figure 1: Ratios of hadron masses over F_π , as a function of the fermion mass in units of F_π , from Ref. [2]. (Figure courtesy of E. Neil.)

the lattice spacing by computing values for the low-energy constant $a\hat{B}_\pi$ in lattice units. From the fourth line of Eq. (2.4) one obtains $v(m)$, and then from the second line of Eq. (2.3) one computes $a\hat{B}_\pi$. Doing this, we find that this quantity is constant to within 3% over the range of fermion masses considered in the numerical simulations, which is well within the errors on the computed values at each am . This validates our assumption that the lattice spacing does not depend on m .

3. Taste breaking

The simulations of Refs. [1, 2] were performed with staggered fermions, and Ref. [2] reported, in addition to the “exact” NG pion mass M_π also the values for the “taste” pions M_{i5} and M_{ij} . Mass-squared differences are shown in Fig. 2. Both taste splittings show a strong dependence on the fermion mass at fixed lattice spacing. This is very much unlike QCD, where, if one plots the differences between the squares of the masses of the different tastes, one would find virtually no dependence on the fermion mass, *i.e.*, horizontal lines (see, for example, Fig. 3 in Ref. [10]).

An important question is whether the dChPT framework can explain this salient difference, which has also been observed in the $SU(3)$ theory with two sextet fermions [11]. In staggered QCD, taste splittings can be understood in terms of staggered ChPT [12, 13] (for reviews, see Refs. [10, 14]). In the Symanzik effective action, the leading-order taste-breaking effects are encapsulated by four-fermion operators of the form [12]

$$a^2(\bar{\psi}\Gamma\psi)(\bar{\psi}\Gamma\psi), \quad (3.1)$$

where Γ is a gamma-matrix acting on the taste index of ψ . The operator $(\bar{\psi}\Gamma\psi)(\bar{\psi}\Gamma\psi)$ has an

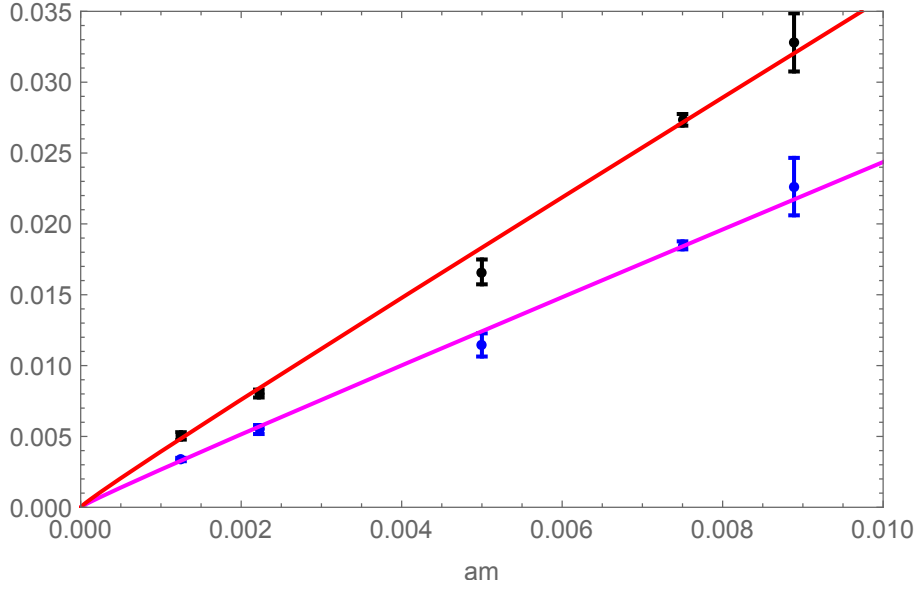


Figure 2: Taste splittings $(aM_{ij})^2 - (aM_\pi)^2$ (black points; red curve), and $(aM_{i5})^2 - (aM_\pi)^2$ (blue points; magenta curve), as a function of am . Data from Ref. [2].

anomalous dimension γ_Γ , and thus transforms under a scale transformation with parameter λ as

$$(\bar{\psi}\Gamma\psi)(\bar{\psi}\Gamma\psi) \rightarrow \lambda^{6-\gamma_\Gamma} (\bar{\psi}\Gamma\psi)(\bar{\psi}\Gamma\psi), \quad (3.2)$$

which leads us to introduce a spurion field for a^2 transforming as $a^2 \rightarrow \lambda^{-2+\gamma_\Gamma} a^2$. It follows that the operator (3.1) is represented in dChPT as

$$c_\Gamma a^2 \hat{f}_\pi^6 e^{(6-\gamma_\Gamma)\tau} \text{tr}(\Sigma\Gamma\Sigma^\dagger\Gamma), \quad (3.3)$$

where now Γ acts on the taste index of Σ [12, 13, 10], and c_Γ is a dimensionless low-energy constant.³ Since there is more than one possible choice for Γ , we find from Eq. (3.3) that

$$(aM_\Gamma)^2 - (aM_\pi)^2 = (af_\pi)^4 \sum_{\Gamma'} c_{\Gamma'} e^{(4-\gamma_{\Gamma'})v(m)}. \quad (3.4)$$

Assuming, as is the case for QCD, that one operator dominates leads to the simpler expression

$$(aM_\Gamma)^2 - (aM_\pi)^2 = A_\Gamma e^{(4-\gamma_\Gamma)v(m)}, \quad (3.5)$$

and this is the expression we fit to the data, yielding the red and magenta curves in Fig. 2. The values of the fit parameters are

$$\begin{aligned} A_{i5} &= 2.0 \times 10^{-6}, & \gamma_{i5} &= 1.9, \\ A_{ij} &= 2.9 \times 10^{-6}, & \gamma_{ij} &= 1.9. \end{aligned} \quad (3.6)$$

³In staggered ChPT both single- and double-trace operators appear, but only single-trace operators contribute to the taste splittings at leading order.

As these fits are preliminary, we did not yet estimate errors. We note, however, that the fits yield $\gamma_{i5} \simeq \gamma_{ij} \approx 2\gamma_*$. A more complete analysis is in preparation. However, it is clear that dChPT has a feature not present in standard ChPT: the appearance of powers of $e^{\nu(m)}$ in tree-level results. These factors explain why the taste splittings are strongly dependent on the fermion mass to leading order in dChPT at a fixed lattice spacing, in the large-mass regime. This is in sharp contrast with what happens in QCD with staggered fermions, where taste splittings are independent of the fermion mass to leading order (and, to a very good precision, in simulations). The different slopes seen in Fig. 2 are explained by the different values of A_{i5} and A_{ij} found in the fits.

4. Concluding remarks

In this preliminary investigation of the LSD data for the 8-flavor $SU(3)$ theory using tree-level dChPT, we find that, at least semi-quantitatively, lowest-order dChPT describes the data quite well. In particular, dChPT appears to be able to describe the taste-splitting pattern in staggered discretizations of this theory, which shows a very different pattern from that of staggered lattice QCD. We take this as a sign that the description of the low-energy behavior of this theory using dChPT is on the right track.

A complete leading-order analysis of the data is in progress [9]. While this is a natural starting point, of course NLO effects should eventually be considered as well.⁴

From our analysis, we can conclude that if indeed dChPT is the correct low-energy effective theory, the simulations of Refs. [1, 2, 3] are in the “large-mass” regime [7], in which the data show approximate hyperscaling. The intuitive understanding is that the fermion mass m is large enough to dominate the breaking of scale invariance. If this is the case, that would make it more difficult to settle the question whether indeed (as assumed here) the 8-flavor $SU(3)$ theory is just outside, or already inside, the conformal window.

Given that it is expensive to enlarge the (linear) volume L (while keeping the lattice spacing fixed), another way of avoiding the large-mass regime would be to make the fermion mass m smaller. This would possibly drive the pions in the theory into the ε -regime [8]. This regime is also accessible to dChPT [19]. However, values of F_π would be much closer to \hat{f}_π , which is predicted by dChPT to be very small, and it might not be easy to satisfy the requirement that $F_\pi L \gtrsim 1$.

Acknowledgements

We would like to thank Ethan Neil for discussions and extensive communication about the data, and Julius Kuti for discussions. This work was supported in part by the U.S. Department of Energy under grant DE-SC0013682 (SFSU) and by the Israel Science Foundation under grant no. 491/17 (Tel Aviv).

References

- [1] T. Appelquist *et al.*, Phys. Rev. D **93**, no. 11, 114514 (2016) [arXiv:1601.04027 [hep-lat]].
- [2] T. Appelquist *et al.* [Lattice Strong Dynamics Collaboration], arXiv:1807.08411 [hep-lat].

⁴For some work in this direction, not necessarily within dChPT, see Refs. [15, 16, 17, 18].

- [3] Y. Aoki *et al.* [LatKMI Collaboration], Phys. Rev. D **96**, no. 1, 014508 (2017) [arXiv:1610.07011 [hep-lat]].
- [4] M. Golterman and Y. Shamir, Phys. Rev. D **94**, no. 5, 054502 (2016) [arXiv:1603.04575 [hep-ph]].
- [5] M. Golterman and Y. Shamir, PoS LATTICE **2016**, 205 (2016) [arXiv:1610.01752 [hep-ph]].
- [6] M. Golterman and Y. Shamir, Phys. Rev. D **95**, no. 1, 016003 (2017) [arXiv:1611.04275 [hep-ph]].
- [7] M. Golterman and Y. Shamir, Phys. Rev. D **98**, no. 5, 056025 (2018) [arXiv:1805.00198 [hep-ph]].
- [8] Z. Fodor, K. Holland, J. Kuti and C. H. Wong, PoS LATTICE **2018**, 196 (2019) [arXiv:1901.06324 [hep-lat]].
- [9] M. Golterman, E. Neil and Y. Shamir, work in progress.
- [10] M. Golterman, arXiv:0912.4042 [hep-lat].
- [11] Z. Fodor, K. Holland, J. Kuti, D. Nogradi, C. Schroeder and C. H. Wong, Phys. Lett. B **718**, 657 (2012) [arXiv:1209.0391 [hep-lat]].
- [12] W. J. Lee and S. R. Sharpe, Phys. Rev. D **60**, 114503 (1999) [hep-lat/9905023].
- [13] C. Aubin and C. Bernard, Phys. Rev. D **68**, 034014 (2003) [hep-lat/0304014].
- [14] A. Bazavov *et al.* [MILC Collaboration], Rev. Mod. Phys. **82**, 1349 (2010) [arXiv:0903.3598 [hep-lat]].
- [15] T. Appelquist, J. Ingoldby and M. Piai, JHEP **1803**, 039 (2018) [arXiv:1711.00067 [hep-ph]].
- [16] T. Appelquist, J. Ingoldby and M. Piai, arXiv:1908.00895 [hep-ph].
- [17] M. Hansen, K. Langæble and F. Sannino, Phys. Rev. D **95**, no. 3, 036005 (2017) [arXiv:1610.02904 [hep-ph]].
- [18] O. Catà and C. Müller, arXiv:1906.01879 [hep-ph].
- [19] T. V. Brown, M. Golterman, S. Krøjer, Y. Shamir and K. Splittorff, arXiv:1909.10796 [hep-lat].